The *GW* approximation: A quantum chemistry perspective

Antoine Marie, Abdallah Ammar, and Pierre-François Loos*
Laboratoire de Chimie et Physique Quantiques (UMR 5626), Université de Toulouse, CNRS, UPS, Toulouse, France
*Corresponding author. e-mail address: loos@irsamc.ups-tlse.fr

Contents

Abstract

We provide an in-depth examination of the *GW* approximation of Green's function many-body perturbation theory by detailing both its theoretical and practical aspects in the realm of quantum chemistry. First, the quasiparticle context is introduced before delving into the derivation of Hedin's equations. From these, we explain how to derive the well-known *GW* approximation of the self-energy. In a second time, we meticulously explain each step involved in a *GW* calculation and what type of physical quantities can be computed. To illustrate its versatility, we consider two contrasting systems: the water molecule, a weakly correlated system, and the carbon dimer, a strongly correlated system. Each stage of the process is thoroughly detailed and explained alongside numerical results and illustrative plots. We hope that the contribution will facilitate the dissemination and democratization of Green's function-based formalisms within the computational and theoretical quantum chemistry community.

1. Quasiparticles

The concept of quasiparticles stands as the cornerstone of many-body perturbation theory, serving as a vital tool for characterizing the intricate

Advances in Quantum Chemistry
ISSN 0065-3276, https://doi.org/10.1016/bs.aiq.2024.04.001

behaviors of particles within a complex quantum many-body system.[1] Quasiparticles allow, for example, to elucidate the collective behavior of the underlying particles while staying in a single-particle picture. This is achieved by "dressing" the particles of interest with the complex many-body effects to create fictitious particles. Despite being treated within a single-particle framework, these quasiparticles encapsulate correlation through their dressing.

To illustrate this, consider the example of the removal or addition of an electron. In a single-particle framework, like Hartree-Fock (HF) theory, the electrons are perceived as independent entities. According to Koopmans' theorem, the energy needed to extract one electron from the system is merely the negative of its one-particle energy, denoted as $-\varepsilon$. However, this depiction assumes that the act of withdrawing an electron has no impact on the surrounding electrons, which, of course, is far from accurate.

A more realistic perspective portrays the removal of an electron as likely to perturb its neighboring electrons, giving rise to minor disruptions. These disturbances manifest as neutral excitations, maintaining the total number of particles, yet elevating some electrons to higher-energy one-particle states due to the removal of the targeted electron. In the quasiparticle framework, these neutral excitations are dressed on the electron transforming it into a "quasielectron" with distinct properties compared to its bare counterpart (as illustrated in Fig. 1). For example, the interaction between two quasielectrons is characterized by a screened Coulomb interaction because the dressing effectively "shields" or "screens" each particle.

Consequently, in a single-particle treatment, the energy required to extract this quasielectron becomes $-\varepsilon - \Sigma$, where Σ represents the so-called self-energy of the quasiparticle. Thus, even when quasiparticles are considered independently from the rest of the system, the removal energy takes into account many-body effects between real particles through the contribution of the self-energy. This concept similarly applies to the electron addition process.

In essence, quasiparticles enable a more accurate portrayal of how particles in a many-body quantum system interact and influence one another, shedding light on their collective behavior and dynamic responses to perturbations.

The *GW* approximation of Green's function many-body perturbation theory, which is discussed in detail in the following, aims to provide a

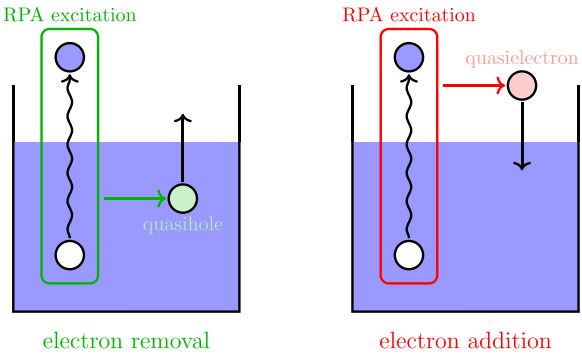

Fig. 1 Schematic representation of an electron removal (left) and electron addition (right) process within the *GW* approximation: the bare hole (white) and the bare electron (blue) are "dressed" by the RPA neutral excitations and then become a quasihole (green) and a quasielectron (red).

detailed description of the electronic structure and spectral properties of materials and molecules by utilizing the one-body Green's function. It makes extensive use of the quasiparticle concept via the construction of a dynamically-screened version of the Coulomb interaction.[2] *GW* has been particularly successful in condensed matter physics and has emerged as a highly valuable tool for computing excited-state properties such as band-gaps and band-edge energy levels. We refer the interested reader to Refs.[3–6] for an in-depth discussion of *GW* (and beyond). The book of Martin, Reining, and Ceperley[7] is a particularly valuable resource, especially for those newly venturing into this field (see also Refs. [8-9]).

Within this context, we propose a more "quantum chemical" perspective on the *GW* approximation. First, we provide a detailed derivation of the *GW* equations, as outlined in Sec. 2. Then, we present concrete numerical examples involving typical molecular systems exhibiting both weak and strong correlations (see Sec. 3). The content featured in these sections aims to facilitate the implementation of *GW* within existing quantum chemistry software, bridging the gap between theory and practical applications.

2. *GW* in theory

The primary objective of the *GW* method is to approximate the exact one-body Green's function

$$G(11') = (-\mathrm{i})\langle \Psi_0^N \,|\hat{T}[\hat{\psi}(1)\hat{\psi}^\dagger(1')]|\, \Psi_0^N\rangle \tag{1}$$

where Ψ_0^N is the exact N-electron ground-state wave function, $\hat{T}$ is the time-ordering operator, and $1 = (t_1, x_1) = (t_1, \sigma_1, r_1)$ is a time-spin-space composite index. $\hat{\psi}(1)$ and $\hat{\psi}^\dagger(1')$ are second-quantized annihilation and creation field operators in the Heisenberg picture, respectively, that are related to their counterparts in the Schrödinger picture as follows

$$\hat{\psi}(1) = e^{i\hat{H}t_1}\hat{\psi}(\mathbf{x_1})e^{-i\hat{H}t_1} \tag{2}$$

Because the electronic Hamiltonian $\hat{H}$ is time-independent, it is easy to show that $G(11')$ depends only on the time difference $t_1 - t_{1'}$.

The one-body Green's function gives access to the charged excitation energies of the system through its poles in the complex plane as can be readily seen by its Lehmann representation

$$G(\boldsymbol{x}_1\boldsymbol{x}_{1'};\omega) = \sum_S \frac{\mathcal{I}_S(\boldsymbol{x}_1)\mathcal{I}_S^*(\boldsymbol{x}_{1'})}{\omega - (E_0^N - E_S^{N-1}) - i\eta} + \sum_S \frac{\mathcal{A}_S(\boldsymbol{x}_1)\mathcal{A}_S^*(\boldsymbol{x}_{1'})}{\omega - (E_S^{N+1} - E_0^N) + i\eta} \tag{3}$$

where η is a positive infinitesimal, E_0^N is the ground-state energy of the N-electron system, while E_S^{N+1} and E_S^{N-1} are the Sth excited-state energies of the $(N-1)$- and $(N+1)$-electron systems, respectively. The numerators

$$\mathcal{I}_S(\boldsymbol{x}) = \langle \Psi_S^{N-1}|\hat{\psi}(\boldsymbol{x})|\Psi_0^N\rangle \tag{4a}$$

$$\mathcal{A}_S(\boldsymbol{x}) = \langle \Psi_0^N|\hat{\psi}(\boldsymbol{x})|\Psi_S^{N+1}\rangle \tag{4b}$$

are known as the Lehmann amplitudes or Dyson orbitals.

The success of the GW approximation (and of any other approximations based on Green's functions) hinges on the ability to compute G without explicit reference to the many-body wave function. This remarkable property is made possible through a closed set of equations known as Hedin's equations.[2] In the following, we give the outline of their derivation, while a more comprehensive derivation is provided as supporting information. Note that, here, we rely on four-point quantities to derive Hedin's equations.[10–13] We refer the interested reader to Refs. [6,7,14] for details about the usual two-point version.

The initial step of this derivation consists of writing down the equation of motion of the one-body Green's function

$$\int \mathrm{d}3\left[\mathrm{i}\delta(13)\frac{\partial}{\partial t_3} - h(13)\right] G(31') + \mathrm{i}\int \mathrm{d}(232')\, v(12;\, 32')\, G_2(32'^{+};\, 1'2^{++}) = \delta(11') \tag{5}$$

This equation establishes a connection between G and the two-body Green's function, defined as

$$G_2(12;\, 1'2') = (-\mathrm{i})^2 \langle \Psi_0^N | \hat{T}\left[\hat{\psi}(1)\hat{\psi}(2)\hat{\psi}^\dagger(2')\hat{\psi}^\dagger(1')\right] | \Psi_0^N \rangle \tag{6}$$

Here, $h(12)$ is the one-body part of the Hamiltonian, $\delta(12) = \delta(t_1 - t_2)\delta(\boldsymbol{x}_1 - \boldsymbol{x}_2)$ is the Dirac delta function, and $1^\pm = (t_1 \pm \eta, \boldsymbol{x}_1)$. Additionally, the four-point Coulomb interaction is given by

$$v(12;\, 34) = \delta(\boldsymbol{x}_1 - \boldsymbol{x}_3)\frac{\delta(t_1 - t_2)}{|\boldsymbol{r}_1 - \boldsymbol{r}_2|}\delta(\boldsymbol{x}_2 - \boldsymbol{x}_4) \tag{7}$$

The equation of motion associated with G_2 would link the two- and three-body Green's functions. However, this path does not lead to a closed set of equations for G, which is our primary objective.

To proceed, we reframe the equation of motion presented in Eq. (5) as a Dyson equation

$$G(11') = G_0(11') + \int \mathrm{d}(23)\, G_0(12)\Sigma(23)\, G(31') \tag{8}$$

by introducing the self-energy

$$\Sigma(11') = -\mathrm{i}\int \mathrm{d}(232'3')\, v(12;\, 3'2')\, G_2(3'2'^{+};\, 32^{++})\, G^{-1}(31') \tag{9}$$

and the non-interacting one-body Green's function

$$\int \mathrm{d}3\left[\mathrm{i}\delta(13)\frac{\partial}{\partial t_3} - h(13)\right] G_0(31') = \delta(11') \tag{10}$$

Then, the next step is to express the self-energy in terms of G and the crucial element for this task is the Martin-Schwinger relation[15]

$$\left.\frac{\delta G(11';\, [U])}{\delta U(2'2)}\right|_{U=0} = -G_2(12;\, 1'2') + G(11')\, G(22') \tag{11}$$

which express G_2 in terms of the derivative of the one-body Green's function with respect to a fictitious external potential U. The equilibrium

Green's function is retrieved by taking the limit $U \to 0$, i.e., $G(11'; [U = 0]) = G(11')$. In the following, to lighten the notations, we omit the functional dependence in U and the corresponding limit. The second term in the right-hand side of Eq. (11) leads to the Hartree (H) part of the self-energy

$$\Sigma_{\text{H}}(11') = -\text{i}\delta(11') \int \text{d}(22')\, v(12; 1'2')\, G(2'2^+) \tag{12}$$

and the remaining term encapsulates all the exchange-correlation (xc) effects, which reads, after some manipulation,

$$\Sigma_{\text{xc}}(11') = \text{i} \int \text{d}(22'33')\, G(33')\, W(12'; 32)\, \tilde{\Gamma}(3'2; 1'2') \tag{13}$$

In Eq. (13), the dynamically-screened Coulomb interaction W is also defined through a Dyson equation

$$W(12; 1'2') = v(12^-; 1'2') - \text{i} \int \text{d}(343'4')\, W(14; 1'4')\, \tilde{L}(3'4'; 3^+4)\, v(23; 2'3') \tag{14}$$

which kernel is the "irreducible" polarizability

$$\tilde{L}(12; 1'2') = \int \text{d}(33')\, G(13)\, G(3'1')\, \tilde{\Gamma}(32; 3'2') \tag{15}$$

The missing ingredient to close Hedin's equations is the four-point "irreducible" vertex function

$$\tilde{\Gamma}(12; 1'2') = \delta(12')\delta(1'2) + \int \text{d}(33'44')\, \Xi_{\text{xc}}(13'; 1'3)\, G(34)\, G(4'3')\, \tilde{\Gamma}(42; 4'2') \tag{16}$$

where

$$\Xi_{\text{xc}}(12'; 1'2) = \frac{\delta \Sigma_{\text{xc}}(11')}{\delta G(22')} \tag{17}$$

is the exchange-correlation kernel.

We are now in a position to derive the GW approximation. Neglecting the so-called vertex effects by only considering the first term in Eq. (16),

that is, $\tilde{\Gamma}(12;\,1'2') \approx \delta(12')\delta(1'2)$, yields the following form of the self-energy

$$\Sigma_{\mathrm{xc}}^{GW}(11') = \mathrm{i}\int \mathrm{d}(22')\, G(22')\, W(2'1;\,1'2) \tag{18}$$

which gives its name to this particular approximation. It is worth noting that since $\tilde{\Gamma}$ also plays a role in the polarizability, as seen in Eq. (15), one has the flexibility to choose whether to apply the same approximation or to opt for an alternative. This choice results in different forms of the *GW* self-energy.[11,14,16–32] However, the most common and natural approach is to use the same approximation of $\tilde{\Gamma}$ for both the self-energy and the polarizability. In this case, the irreducible polarizability reads

$$\tilde{L}(1'2';\,12) = G(1'2)\, G(2'1) \tag{19}$$

and the correponding reducible polarizability

$$L(12;\,1'2') = \tilde{L}(12;\,1'2') - \mathrm{i}\int \mathrm{d}(33'44')\, \tilde{L}(13;\,1'3')\, v(3'4';\,34)\, L(42;\,4'^{+}2') \tag{20}$$

is the well-known random-phase approximation (RPA).[33–36] Consequently, *GW* can be regarded as the first-order approximation of the self-energy with respect to the screened interaction within which the dynamical screening is computed at the RPA level.

Note that here we focus on Hedin's equation, that is, a closed set of equations in terms of the screened interaction. However, an analogous set of equations in terms of the Coulomb interaction can be derived. This alternative set is also derived in the supporting information for the sake of completeness.

3. *GW* in practice

In this section, we propose to explain the various processes involved in a *GW* calculation and what type of physical quantities can be computed, and at which step. As examples, we consider one weakly correlated system, the water molecule H_2O, and one strongly correlated system, the carbon dimer C_2. Their geometry has been extracted from the QUEST database.[37–39] By strong correlation, we mean that several electronic states are close in energy to each other (near degeneracy effects). In this case, a

multireference treatment might be more appropriate, but one can also employ a single-reference formalism and hope that the post-treatment is accurate enough to compensate for the poor choice of reference configuration. For both closed-shell systems, we consider Dunning's aug-cc-pVTZ basis set. All *GW* calculations are initiated from HF quantities computed in the restricted formalism.[40] All the orbitals are corrected within our scheme and, unless otherwise stated, we set $\eta = 0$. Note that the *GW* method can be used to correct any mean-field calculations and it is common practice to "tune" the starting point using Kohn-Sham orbitals and energies with the "right" functional. However, for the sake of simplicity, we shall not consider nor discuss this point in the present review (see, e.g., Refs. [23,29,41–44] for illustrative examples).

All the *GW* calculations reported in the present section have been performed with QUACK, an open-source software for emerging quantum electronic structure methods, which source code is available at https://github.com/pfloos/QuAcK. Implementations of *GW* methods for localized basis sets are available in several software, such as FIESTA,[45,46] BEDEFT,[47,48] MOLGW,[49] TURBOMOLE,[50–53] ADF,[32,54–56] FHI-AIMS.[57–60] EXCITON+[61–64] and PYSCF.[65–67]

Throughout this section, we assume real spinorbitals which is usually the case in molecular calculations, unless a magnetic field is considered.[68] The indices i, j, k, and l are occupied (hole) orbitals; a, b, c, and d are unoccupied (particle) orbitals; p, q, r, and s indicate arbitrary orbitals; m labels single excitations/deexcitations; and μ, ν, λ, and σ denote basis functions.

3.1 *GW* self-energy

In practice, the first step toward obtaining the self-energy is to compute the polarizability. As alluded to earlier, the irreducible polarizability $\tilde{L}$, Eq. (19), is employed to calculate W within the *GW* approximation via its link with the reducible polarizability L, Eq. (20), constructed by utilizing the eigenvalues and eigenvectors of the RPA problem.[69–71] The non-Hermitian RPA linear eigenvalue problem is completely defined by the following Casida-like equations expressed in the basis of excitations ($i \to a$) and deexcitations ($a \to i$)

$$\begin{pmatrix} \boldsymbol{A} & \boldsymbol{B} \\ -\boldsymbol{B} & -\boldsymbol{A} \end{pmatrix} \cdot \begin{pmatrix} \boldsymbol{X} & \boldsymbol{Y} \\ \boldsymbol{Y} & \boldsymbol{X} \end{pmatrix} = \begin{pmatrix} \boldsymbol{X} & \boldsymbol{Y} \\ \boldsymbol{Y} & \boldsymbol{X} \end{pmatrix} \cdot \begin{pmatrix} \boldsymbol{\Omega} & \boldsymbol{0} \\ \boldsymbol{0} & -\boldsymbol{\Omega} \end{pmatrix} \tag{21}$$

where the diagonal matrix $\boldsymbol{\Omega}$ contains the positive eigenvalues and the normalization conditions are

$$\boldsymbol{X}^{\mathrm{T}}\cdot\boldsymbol{X} - \boldsymbol{Y}^{\mathrm{T}}\cdot\boldsymbol{Y} = \mathbf{1} \tag{22a}$$

$$\boldsymbol{X}^{\mathrm{T}}\cdot\boldsymbol{Y} - \boldsymbol{Y}^{\mathrm{T}}\cdot\boldsymbol{X} = \mathbf{0} \tag{22b}$$

The matrix elements of the (anti)resonant block $\boldsymbol{A}$ and the coupling block $\boldsymbol{B}$ read

$$A_{ia,jb} = (\epsilon_a - \epsilon_i)\,\delta_{ij}\,\delta_{ab} + \langle ib|aj\rangle \tag{23a}$$

$$B_{ia,jb} = \langle ij|ab\rangle \tag{23b}$$

with

$$\langle pq|rs\rangle = \iint \frac{\phi_p(\boldsymbol{x}_1)\,\phi_q(\boldsymbol{x}_2)\,\phi_r(\boldsymbol{x}_1)\,\phi_s(\boldsymbol{x}_2)}{|\boldsymbol{r}_1 - \boldsymbol{r}_2|}\mathrm{d}\boldsymbol{x}_1\,\mathrm{d}\boldsymbol{x}_2 \tag{24}$$

the usual electron repulsion integrals in the spinorbital basis. One can estimate the correlation energy at the RPA level via the "trace" or "plasmon" RPA formula[72–77]

$$E_{\mathrm{c}}^{\mathrm{RPA}} = \frac{1}{2}\mathrm{Tr}(\boldsymbol{\Omega} - \boldsymbol{A}) \tag{25}$$

In practice, in the absence of instabilities,[78] the linear eigenvalue problem (21) has particle-hole symmetry which means that the eigenvalues are obtained by pairs $\pm\Omega_m$. Hence, Eq. (21) can be recast as a Hermitian problem of half its original dimension thanks to the positive definiteness of $\boldsymbol{A}-\boldsymbol{B}$

$$(\boldsymbol{A} - \boldsymbol{B})^{1/2}\cdot(\boldsymbol{A} + \boldsymbol{B})\cdot(\boldsymbol{A} - \boldsymbol{B})^{1/2}\cdot\boldsymbol{Z} = \boldsymbol{Z}\cdot\boldsymbol{\Omega}^2 \tag{26}$$

with

$$\boldsymbol{X} + \boldsymbol{Y} = (\boldsymbol{A} - \boldsymbol{B})^{+1/2}\cdot\boldsymbol{Z}\cdot\boldsymbol{\Omega}^{-1/2} \tag{27a}$$

$$\boldsymbol{X} - \boldsymbol{Y} = (\boldsymbol{A} - \boldsymbol{B})^{-1/2}\cdot\boldsymbol{Z}\cdot\boldsymbol{\Omega}^{+1/2} \tag{27b}$$

(See the supporting information for a detailed derivation of these expressions.) At the RPA level, instabilities are quite unusual. Indeed, in the case of real spin orbitals, we have $\langle ib|aj\rangle = \langle ij|ab\rangle$, which yields $(\boldsymbol{A} - \boldsymbol{B})_{ia,jb} = (\epsilon_a - \epsilon_i)\delta_{ij}\delta_{ab}$. Therefore, except in the case of unusual orbital occupations, $\boldsymbol{A} - \boldsymbol{B}$ is positive definite. Alternatively, one can enforce the Tamm-Dancoff approximation by setting $\boldsymbol{B} = \mathbf{0}$ but, in this case, one gets $E_{\mathrm{c}}^{\mathrm{RPA}} = 0$, as readily seen in Eq. (25).

Using these quantities, one can compute the elements of the dynamically screened Coulomb interaction as

$$W_{pq,rs}(\omega) = \langle pq|rs\rangle + \sum_m \left[\frac{M_{pr,m} M_{qs,m}}{\omega - \Omega_m + i\eta} - \frac{M_{pr,m} M_{qs,m}}{\omega + \Omega_m - i\eta} \right] \tag{28}$$

where the transition densities (or "screened" two-electron integrals) are given by

$$M_{pq,m} = \sum_{jb} \langle pj|qb\rangle (X_{jb,m} + Y_{jb,m}) \tag{29}$$

Due to the spin structure of the *GW* equations, only the singlet RPA excitations contribute to the transition densities, which is used in practice to further reduce the size of the RPA problem via spin adaptation.[13,77]

It is important to note that one needs to compute the entire spectrum of eigenvalues and their corresponding eigenvectors, as the sum over m in Eq. (28) cannot be truncated to the first few excitations, as commonly performed in linear response calculations via Davidson's algorithm.[79] (We shall get back to this point later on.) Because the RPA matrices [see Eq. (21)] are of size $O(N^2) \times O(N^2)$ (where N is the number of orbitals), this step costs $O(N^6)$ and is thus the computational bottleneck of a *GW* calculation. Important techniques, such as the contour deformation approach, have been designed to leverage this.[47,48,50,55,56,80–87] (See Ref. [6] for an extensive list of the different techniques).

Figure 2 shows the low-frequency part of the absorption spectrum of H_2O and C_2 computed at the RPA/aug-cc-pVTZ level. It has been modeled as a convolution of Gaussian functions centered at each (singlet) neutral excitation frequency Ω_m with intensity proportional to the corresponding oscillator strength of the transition[88]

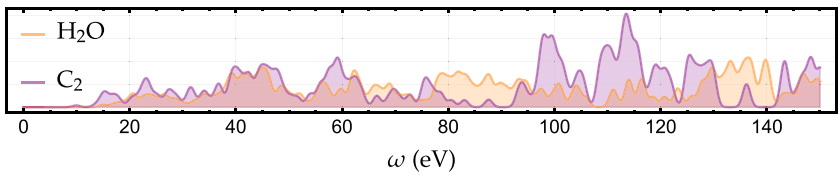

Fig. 2 Low-frequency part of the absorption spectrum of H_2O (orange) and C_2 (purple) computed at the RPA level with the aug-cc-pVTZ basis. See main text for more details.

$$f_m = \frac{2}{3}\Omega_m \|\boldsymbol{\mu}_m\|^2 \tag{30}$$

where the transition dipole moment is

$$\boldsymbol{\mu}_m = \sum_{ia} \langle i|\boldsymbol{r}|a\rangle (X_{ia,m} + Y_{ia,m}) \tag{31}$$

and

$$\langle p|\boldsymbol{r}|q\rangle = \int \varphi_p(\boldsymbol{x})\, \boldsymbol{r}\, \varphi_q(\boldsymbol{x})\, \mathrm{d}\boldsymbol{x} \tag{32}$$

are one-electron integrals. Fig. 2 evidences the fine structure of such a quantity and the difficulty of modeling it with the well-known (generalized) plasmon-pole approximation that is widely applied in solid-state calculations,[89] but also in molecular systems.[90,91]

Finally, performing the convolution of the Green's function and the dynamically screened interaction [see Eq. (18)], the elements of the correlation part of the *GW* self-energy read

$$\Sigma^{\mathrm{c}}_{pq}(\omega) = \sum_{im} \frac{M_{pi,m} M_{qi,m}}{\omega - \epsilon_i + \Omega_m - \mathrm{i}\eta} + \sum_{am} \frac{M_{pa,m} M_{qa,m}}{\omega - \epsilon_a - \Omega_m + \mathrm{i}\eta} \tag{33}$$

Note that, in a *GW* calculation, it is not mandatory to compute explicitly the elements of W defined in Eq. (28). Only the transition densities [see Eq. (29)] are required to compute the self-energy elements in Eq. (33).

At this stage, we have not specified the nature of the orbitals and their energies in Eqs. (23a), (23b), (24), and (33) as this choice depends on the level of self-consistency one is willing to include.

3.2 Level of self-consistency

The practical equation to be solved is known as the quasiparticle equation

$$[\boldsymbol{F} + \boldsymbol{\Sigma}^{\mathrm{c}}(\omega = \epsilon_p)]\psi_p(\boldsymbol{x}) = \epsilon_p \psi_p(\boldsymbol{x}) \tag{34}$$

where ϵ_p are the quasiparticle energies and $\psi_p(\boldsymbol{x})$ are the corresponding (Dyson) orbitals. $\boldsymbol{F}$ is the usual Fock matrix and $\boldsymbol{\Sigma}^{\mathrm{c}}(\omega)$ is a matrix with elements derived from Eq. (33). This equation can be interpreted as the HF equation augmented with an additional term that accounts for correlations arising from the screening effect among electrons. Note also the close link with Kohn-Sham density-functional theory. However, the primary challenge in solving this equation stems from the frequency-dependent nature of the self-energy, rendering it a nonlinear and non-Hermitian matrix

equation. As a result, it is common practice to employ approximations to solve the quasiparticle equation.

In the popular one-shot scheme, known as G_0W_0,[92–98] one only considers the diagonal part of the self-energy and performs a single iteration of Hedin's equations (see pseudo-code in Fig. 3). Considering a HF starting point, the quasiparticle energies are thus obtained by solving the non-linear quasiparticle equation for each orbital p

$$\omega - \epsilon_p^{\mathrm{HF}} = \Sigma_{pp}^{\mathrm{c}}(\omega) \tag{35}$$

where ϵ_p^{HF} are the HF one-electron energy of the pth orbital.

It is also practically convenient to linearize this quasiparticle equation by performing a first-order Taylor expansion of the self-energy around the starting point energy, that is, $\omega = \epsilon_p^{\mathrm{HF}}$,

$$\Sigma_{pp}^{\mathrm{c}}(\omega) \approx \Sigma_{pp}^{\mathrm{c}}(\epsilon_p^{\mathrm{HF}}) + (\omega - \epsilon_p^{\mathrm{HF}}) \left. \frac{\partial \Sigma_{pp}^{\mathrm{c}}(\omega)}{\partial \omega} \right|_{\omega=\epsilon_p^{\mathrm{HF}}} \tag{36}$$

yielding

$$\epsilon_p = \epsilon_p^{\mathrm{HF}} + Z_p \Sigma_{pp}^{\mathrm{c}}(\omega = \epsilon_p^{\mathrm{HF}}) \tag{37}$$

where the value of the renormalization factor Z_p gives the spectral weight of the corresponding quasiparticle solution ϵ_p

$$(Z_p)^{-1} = 1 - \left. \frac{\partial \Sigma_{pp}^{\mathrm{c}}(\omega)}{\partial \omega} \right|_{\omega=\epsilon_p^{\mathrm{HF}}} \tag{38}$$

The value of Z_p can easily be shown to be strictly restricted between 0 and 1. This scheme is coined linG_0W_0 in the following and its pseudo-code is given in Fig. 3. When the so-called quasiparticle approximation holds, the weight of the quasiparticle equation is close to unity, while the remaining weight is distributed among the satellite (or shake-up) transitions.

Several levels of self-consistency can be achieved. One common approach is to enforce self-consistency on the quasiparticle energies, a scheme referred to as the "eigenvalue" self-consistent GW (evGW) method.[45,99–102] In the evGW approach, a series of iterations is conducted, during which updates are made solely to the one-electron energies ϵ_p used in defining the RPA matrices [as seen in Eqs. (23a) and (23b)] and the self-energy [see Eq. (33)], while the corresponding orbitals remain unchanged. This represents the simplest and most widely employed self-consistent scheme. The pseudo-code of the evGW procedure is given in Fig. 3.

procedure G_0W_0@HF
  Perform HF calculation to get orbital coefficients $\boldsymbol{c}^{\mathrm{HF}}$ and energies $\boldsymbol{\epsilon}^{\mathrm{HF}}$
  Integral transformation $\langle\mu\nu|\lambda\sigma\rangle \xrightarrow{\boldsymbol{c}^{\mathrm{HF}}} \langle pq|rs\rangle$
  Construct RPA matrices $\boldsymbol{A}$ and $\boldsymbol{B}$ from $\boldsymbol{\epsilon}^{\mathrm{HF}}$ and $\langle pq|rs\rangle$, as defined in Eqs. (23a) and (23b)
  Compute RPA eigenvalues $\boldsymbol{\Omega}$ and eigenvectors $\boldsymbol{X}+\boldsymbol{Y}$ by diagonalizing the linear eigenvalue problem (21)
  Construct screened two-electron integrals M^m_{pq}, as defined in Eq. (29)
  for $p = 1, \ldots, N$ **do**
    Solve the non-linear equation $\omega = \epsilon_p^{\mathrm{HF}} + \Sigma^{\mathrm{c}}_{pp}(\omega)$ using Newton's method starting from $\omega = \epsilon_p^{\mathrm{HF}}$ to get the quasiparticle energy $\epsilon_p^{G_0W_0}$
  end for
end procedure

procedure linG_0W_0@HF
  Perform HF calculation to get orbital coefficients $\boldsymbol{c}^{\mathrm{HF}}$ and energies $\boldsymbol{\epsilon}^{\mathrm{HF}}$
  Integral transformation $\langle\mu\nu|\lambda\sigma\rangle \xrightarrow{\boldsymbol{c}^{\mathrm{HF}}} \langle pq|rs\rangle$
  Construct RPA matrices $\boldsymbol{A}$ and $\boldsymbol{B}$ from $\boldsymbol{\epsilon}^{\mathrm{HF}}$ and $\langle pq|rs\rangle$, as defined in Eqs. (23a) and (23b)
  Compute RPA eigenvalues $\boldsymbol{\Omega}$ and eigenvectors $\boldsymbol{X}+\boldsymbol{Y}$ by diagonalizing the linear eigenvalue problem (21)
  Construct screened two-electron integrals M^m_{pq}, as defined in Eq. (29)
  for $p = 1, \ldots, N$ **do**
    Compute the self-energy element $\Sigma_{pp}(\omega)$ given in Eq. (33) at $\omega = \epsilon_p^{\mathrm{HF}}$
    Compute the renormalization factor Z_p defined in Eq. (38)
    Evaluate the quasiparticle energy $\epsilon_p^{G_0W_0} = \epsilon_p^{\mathrm{HF}} + Z_p \Sigma^{\mathrm{c}}_{pp}(\omega = \epsilon_p^{\mathrm{HF}})$
  end for
end procedure

procedure evGW@HF
  Perform HF calculation to get orbital coefficients $\boldsymbol{c}^{\mathrm{HF}}$ and energies $\boldsymbol{\epsilon}^{\mathrm{HF}}$
  Integral transformation $\langle\mu\nu|\lambda\sigma\rangle \xrightarrow{\boldsymbol{c}^{\mathrm{HF}}} \langle pq|rs\rangle$
  Set $\boldsymbol{\epsilon}^{G_{-1}W_{-1}} = \boldsymbol{\epsilon}^{\mathrm{HF}}$, and $n = -1$
  while $\Delta > \tau$ **do**
    $n \leftarrow n + 1$
    Construct RPA matrices $\boldsymbol{A}$ and $\boldsymbol{B}$ from $\boldsymbol{\epsilon}^{G_nW_n}$ and $\langle pq|rs\rangle$, as defined in Eqs. (23a) and (23b)
    Compute RPA eigenvalues $\boldsymbol{\Omega}$ and eigenvectors $\boldsymbol{X}+\boldsymbol{Y}$ by diagonalizing the linear eigenvalue problem (21)
    Construct screened two-electron integrals M^m_{pq}, as defined in Eq. (29)
    for $p = 1, \ldots, N$ **do**
      Solve the non-linear equation $\omega = \epsilon_p^{\mathrm{HF}} + \Sigma^{\mathrm{c}}_{pp}(\omega)$ using Newton's method starting from $\omega = \epsilon_p^{G_nW_n}$ to get the quasiparticle energy $\epsilon_p^{G_{n+1}W_{n+1}}$
    end for
    $\Delta = \max\left|\boldsymbol{\epsilon}^{G_{n+1}W_{n+1}} - \boldsymbol{\epsilon}^{G_nW_n}\right|$
  end while
end procedure

procedure qsGW
  Perform HF calculation to get orbital coefficients $\boldsymbol{c}^{\mathrm{HF}}$ and energies $\boldsymbol{\epsilon}^{\mathrm{HF}}$
  Set $\boldsymbol{\epsilon}^{G_{-1}W_{-1}} = \boldsymbol{\epsilon}^{\mathrm{HF}}$, $\boldsymbol{c}^{G_{-1}W_{-1}} = \boldsymbol{c}^{\mathrm{HF}}$, and $n = -1$
  while $\Delta > \tau$ **do**
    $n \leftarrow n + 1$
    Integral transformation $\langle\mu\nu|\lambda\sigma\rangle \xrightarrow{\boldsymbol{c}^{G_nW_n}} \langle pq|rs\rangle$
    Construct RPA matrices $\boldsymbol{A}$ and $\boldsymbol{B}$ from $\boldsymbol{\epsilon}^{G_nW_n}$ and $\langle pq|rs\rangle$, as defined in Eqs. (23a) and (23b)
    Compute RPA eigenvalues $\boldsymbol{\Omega}$ and eigenvectors $\boldsymbol{X}+\boldsymbol{Y}$ by diagonalizing the linear eigenvalue problem (21)
    Construct screened two-electron integrals M^m_{pq}, as defined in Eq. (29)
    Evaluate the self-energy elements $\Sigma^{\mathrm{c}}_{pq}(\omega)$ given in Eq. (33) at $\omega = \epsilon_p^{G_nW_n}$ and form $\tilde{\boldsymbol{\Sigma}}^{\mathrm{c}} = [\boldsymbol{\Sigma}^{\mathrm{c}} + (\boldsymbol{\Sigma}^{\mathrm{c}})^{\intercal}]/2$
    Form the Fock matrix $\boldsymbol{F}$ in orbital basis from $\boldsymbol{c}^{G_nW_n}$
    Diagonalize $\boldsymbol{F} + \tilde{\boldsymbol{\Sigma}}$ to get $\boldsymbol{\epsilon}^{G_{n+1}W_{n+1}}$ and $\boldsymbol{c}^{G_{n+1}W_{n+1}}$
    $\Delta = \max\left|\boldsymbol{\epsilon}^{G_{n+1}W_{n+1}} - \boldsymbol{\epsilon}^{G_nW_n}\right|$
    $n \leftarrow n + 1$
  end while
end procedure

Fig. 3 Pseudo-algorithm for each *GW* scheme: G_0W_0@HF, linG_0W_0@HF, ev*GW*@HF, and qs*GW*.

For a more comprehensive self-consistent treatment, the quasiparticle self-consistent *GW* (qs*GW*) scheme can be employed, which extends the self-consistency to the orbitals themselves.[42,52,55,103–107] In this approach, both the one-electron energies and the orbitals are iteratively updated until

convergence is achieved. The procedure involves diagonalizing an effective Fock matrix that incorporates a correlation potential. This potential is derived from a static Hermitian self-energy, expressed as

$$\tilde{\Sigma}^{c}_{pq} = \frac{\Sigma^{c}_{pq}(\epsilon_p) + \Sigma^{c}_{qp}(\epsilon_q)}{2} \tag{39}$$

Recently, we derived, from first-principles, an alternative static Hermitian form for the qsGW self-energy based on the similarity renormalization group (SRG) approach.[107] The pseudo-code of the qsGW procedure is given in Fig. 3. Although qsGW performs self-consistency on the orbitals and the quasiparticle energies, it is not strictly independent of the starting point as it is not unusual to obtain different solutions depending on the initial set of orbitals and energies.

One should not confuse qsGW with the fully self-consistent GW (scGW) approach,[57,59,60,108–111] where one updates the poles and weights of G retaining quasiparticle and satellite energies at each iteration. We shall not address this scheme here.

3.3 Correlation energy

Despite being a one-body quantity, G can be used to compute the energy of the system. The Galitskii-Migdal (GM) functional,[112] which reads

$$E^{\mathrm{GM}} = -\frac{\mathrm{i}}{2} \int \mathrm{d}\boldsymbol{x}_1 \lim_{2 \to 1^+} \left[\mathrm{i}\frac{\partial}{\partial t_1} + h(\boldsymbol{x}_1) \right] G(12) \tag{40}$$

gives the total electronic energy of the system. The correlation energy can thus be extracted from it and is obtained via the convolution of the correlation part of the self-energy and the Green's function as

$$E^{\mathrm{GM}}_{\mathrm{c}} = -\frac{\mathrm{i}}{2} \int_{-\infty}^{\infty} \frac{\mathrm{d}\omega}{2\pi} \int \mathrm{d}\boldsymbol{x}_1 \boldsymbol{x}_3 e^{\mathrm{i}\omega\eta} \Sigma_{\mathrm{c}}(\boldsymbol{x}_1 \boldsymbol{x}_3; \omega) G(\boldsymbol{x}_3 \boldsymbol{x}_1; \omega) \tag{41}$$

which can be recast as

$$E^{\mathrm{GM}}_{\mathrm{c}} = -\sum_{iam} \frac{M^2_{ia,m}}{\epsilon_a - \epsilon_i + \Omega_m} \tag{42}$$

The derivation of the previous equations starting from Eq. (40) is included in the supporting information. In the context of GW, the Galitskii-Migdal functional, which is known to be non-variational and strongly dependent on the quality of G, grossly overestimates the correlation energy in

molecular systems.[57–60,113–117] Meaningful energies are only obtained at full self-consistency[110,118] or by adding higher-order terms.[119]

The Galitskii-Migdal functional is not the only functional based on G available to compute energies. There are two well-known alternatives, the Luttinger-Ward[120] and Klein[121] functionals, which become variational if G satisfies a Dyson equation. These two functionals are equivalent to the Galitskii-Migdal functional if G is obtained through full self-consistency. To calculate the correlation energy at the GW level using these functionals, an additional RPA calculation is performed and the correlation energy is evaluated via Eq. (25) using the corresponding GW quantities.[113,122–127] (See Ref. [60] for a detailed derivation).

3.4 Quasiparticle energies

Here, we compute the principal ionization potential (IP), I^N, principal electron affinity (EA), A^N, and fundamental gap ($E_g^{\text{fun}} = I^N - A^N$), as depicted in Fig. 4. At the GW level, these quantities are simply given by

$$I^N \approx -\epsilon^{GW}_{\text{HOMO}} \quad A^N \approx -\epsilon^{GW}_{\text{LUMO}} \tag{43}$$

where HOMO and LUMO stand for the highest-occupied and lowest-unoccupied molecular orbitals, respectively.

The black curves in Fig. 5 correspond to the variation of the G_0W_0 self-energy associated with the HOMO and LUMO orbitals of H_2O and C_2 as a function of ω, while the colored lines correspond to $\omega - \epsilon_p^{\text{HF}}$. Therefore, the solutions of the diagonal quasiparticle Eq. (35) can be found where the black and colored curves intersect. Their respective spectral weight is directly related to the slope of the self-energy at these specific intersections.

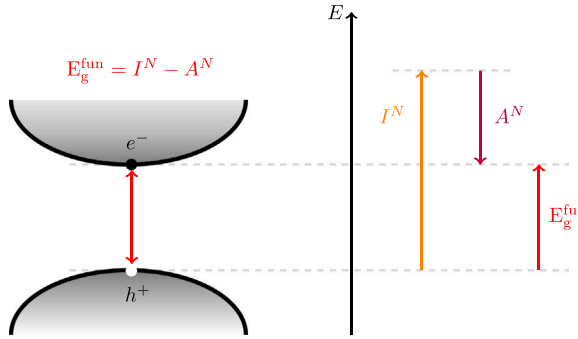

Fig. 4 Fundamental gap $E_g^{\text{fun}} = I^N - A^N$, where I^N and A^N are the principal ionization potential and the principal electron affinity of the N-electron system.

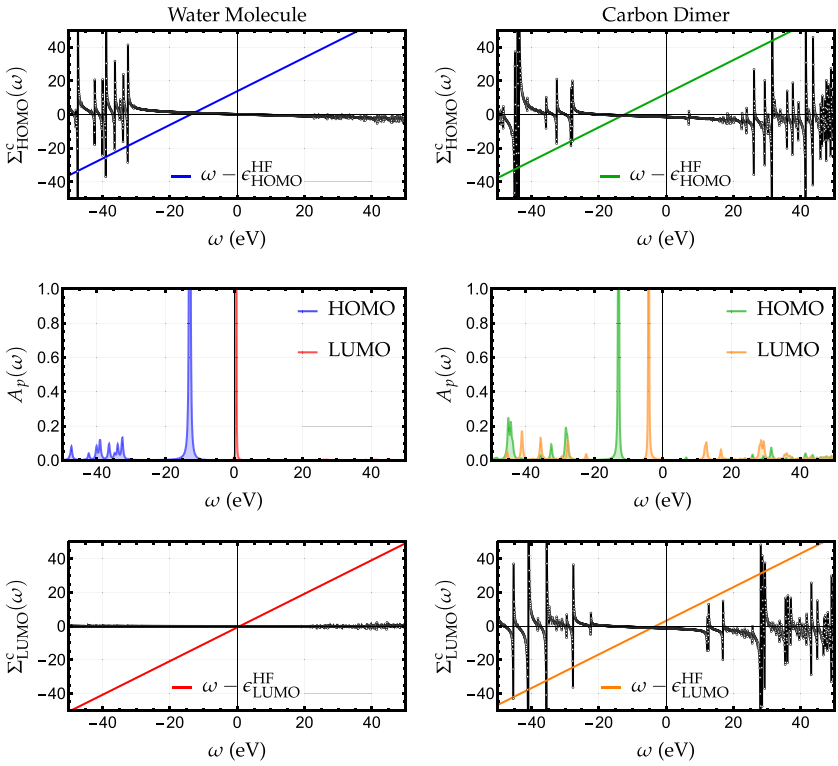

Fig. 5 Self-energy (black curves) associated with the HOMO (top) and LUMO (bottom) orbitals of H_2O (left) and C_2 (right) computed at the G_0W_0 level of theory with the aug-cc-pVTZ basis and $\eta = 10^{-3} E_h$. The solutions of the quasiparticle equation are given by the intersection of the black and colored curves. In the central panels, the spectral function (in E_h^{-1}) associated with the HOMO and LUMO orbitals are represented.

When the slope is small, the renormalization factor is close to unity [see Eq. (38)] and the solution is categorized as a quasiparticle. In the scenario where the slope is high, the renormalization factor is small and the solution corresponds to a satellite. As illustrated in Fig. 5, satellite solutions typically originate from poles in the self-energy. In all the cases depicted in Fig. 5, there is a well-defined quasiparticle solution, clearly separated from the region where the self-energy poles are located. However, it is not uncommon to encounter situations where the weight is almost equally distributed between two solutions.[47,91,118,128–130] In such a case, one can refer to a breakdown of the quasiparticle picture.

One can gain a deeper understanding of how spectral weight is distributed among multiple solutions by examining the spectral function linked to each orbital p. This spectral function, as evidenced by the following equation, is intricately connected to the imaginary part of the one-body Green's function

$$\begin{aligned} A_p(\omega) &= \frac{1}{\pi}|\mathrm{Im}G_{pp}(\omega)| \\ &= \frac{1}{\pi}\frac{|\mathrm{Im}\Sigma^{\mathrm{c}}_{pp}(\omega)|}{[\omega - \epsilon_p^{\mathrm{HF}} - \mathrm{Re}\Sigma^{\mathrm{c}}_{pp}(\omega)]^2 + [\mathrm{Im}\Sigma^{\mathrm{c}}_{pp}(\omega)]^2} \end{aligned} \tag{44}$$

Figure 5 reports $A_{\mathrm{HOMO}}(\omega)$ and $A_{\mathrm{LUMO}}(\omega)$ for both systems. As one can see, it is clear that the quasiparticle solution carries most of the weight in these two specific examples.

The *GW* results for the IP, EA, and fundamental gap obtained at various levels of self-consistency are reported in Table 1. They are compared with the exact results, computed in the same basis set, through full configuration interaction (FCI) calculations on the cationic, anionic, and neutral species.[131] Additionally, Table 1 includes the RPA and Galitskii-Migdal correlation energies [see Eqs. (25) and (42)]. It is clear that the RPA estimates are in much better agreement with the FCI reference values than the Galitskii-Migdal correlation energies which are significantly lower (approximately by a factor of two) and exhibit larger fluctuations with respect to the level of self-consistency, in line with our earlier discussion in Sec. 3.3.

As anticipated, the *GW* estimates for the IP of water are fairly accurate, while the EA of water is found to be negative. Hence, *GW* is not suited to model such an unstable anion. In contrast, the carbon dimer has a stable anionic state, and although C_2 is a prototypical strongly correlated system characterized by a substantial configuration mixing in the N-electron ground state (the weight of the HF reference determinant being only 0.69 in the ground-state FCI wave function), the IP and EA values obtained at the *GW* level are satisfactory.[133,134]

A point worth mentioning is that the linearization of the quasiparticle Eq. (35) is usually an outstanding approximation. This is clearly exemplified here with errors below 0.001 eV for H_2O and C_2. Actually, if one observes a substantial disparity between the linG_0W_0@HF and linG_0W_0 numbers, it might indicate a potential issue, raising concerns about the

Table 1 Principal IP (I^N), principal EA (A^N), fundamental gap ($E_g^{fun} = I^N - A^N$), in units of eV, and RPA and Galitskii-Migdal correlation energies (E_c^{RPA} and E_c^{GM}), in units of E_h, for H_2O and C_2 computed at various levels of theory with the aug-cc-pVTZ basis. The corresponding FCI values and a selection of experimental measurements are reported for the sake of comparison.

Mol.		linG_0W_0 @HF	G_0W_0 @HF	evGW@HF	qsGW[a]	FCI[b]	Exp.[c]
H_2O	I^N	12.885	12.884	12.764	12.879	12.679	12.600
	A^N	−0.685	−0.685	−0.681	−0.662	−0.608	
	E_g^{fun}	13.570	13.569	13.446	13.541	13.287	
	E_c^{RPA}	−0.343	−0.345	−0.348	−0.358	−0.298	
	E_c^{GM}	−0.615	−0.615	−0.631	−0.647		
C_2	I^N	12.928	12.928	12.953	12.561	12.463	11.4 ± 0.3
	A^N	4.153	4.153	4.229	3.840	3.175	3.273 ± 0.008
	E_g^{fun}	8.775	8.775	7.914	8.722	9.288	
	E_c^{RPA}	−0.395	−0.399	−0.401	−0.423	−0.416	
	E_c^{GM}	−0.685	−0.685	−0.699	−0.730		

[a]Calculations performed with SRG regularization and a flow parameter $s = 500$, as described in Ref.[107] [b]Calculations performed with QUANTUM PACKAGE (freely available at https://github.com/QuantumPackage/qp2) using the *"Configuration Interaction using a Perturbative Selection made Iteratively"* (CIPSI) method.[131] [c]Values extracted from the *Computational Chemistry Comparison and Benchmark DataBase* (CCCBDB)[132] at https://cccbdb.nist.gov.

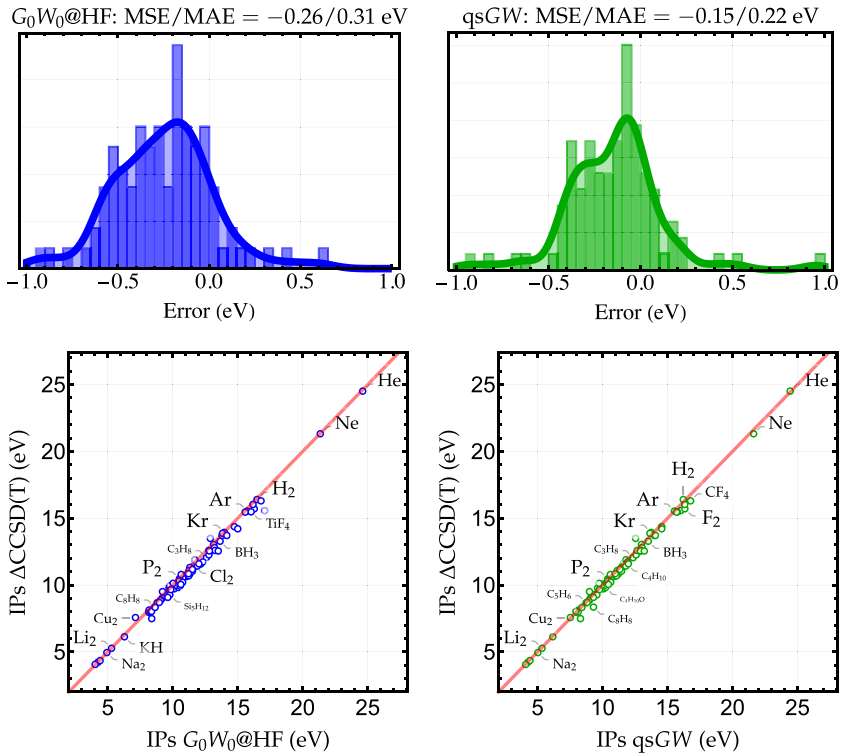

Fig. 7 Histograms (top) and scatter plots (bottom) of the errors in the principal IPs of the *GW*100 dataset [91] computed at the G_0W_0@HF and qs*GW* levels considering the ΔCCSD(T) values of Ref. [53] as reference. Data for G_0W_0@HF and qs*GW* have been extracted from Ref. [135] and are available at https://gw100.wordpress.com. The mean signed error (MSE) and mean absolute error (MAE) with respect to the reference values are also reported.

validity of the quasiparticle approximation. In such situations, it may be prudent to closely examine the spectral function and check for the presence of additional close-lying solutions with significant weight.

Let us return quickly to the RPA problem. In Sec. 3.1, we mentioned that one must compute the entire spectrum of eigenvalues and eigenvectors to obtain well-converged quasiparticle energies. This is illustrated in Fig. 6 where we show the evolution of the quasiparticle energy associated with the HOMO of H_2O and C_2 with respect to the percentage of RPA excitations taken into account in Eq. (28). From this, it is clear that the convergence is quite erratic and non-monotonic, and it is thus hard to design an approximate model with a limited number of poles for the RPA polarizability.

Overall, self-consistency has a beneficial effect in finite systems like atoms and molecules, where both partially and fully self-consistent GW methods have exhibited significant promise.[45,46,54,57–60,101,106–108,136,137] Conversely, the situation is more contentious in solid-state calculations, as the self-consistency and vertex corrections are recognized to offset each other to a certain extent.[7] The debate surrounding the significance of partial and full self-consistency in the GW method has persisted for a long time.[57–60,84,108,113,127,138] In certain scenarios, it has been observed that self-consistency can actually degrade spectral properties when compared to the simpler one-shot G_0W_0 approach. This phenomenon was notably demonstrated in the context of calculations on the uniform electron gas,[139–142] a fundamental model with relevance to many fields of physics and chemistry.[143] Such observations were further confirmed in real extended systems[144–147] It is important to acknowledge that other approximations might have contributed to this deterioration, such as the use of pseudo-potentials[148] or finite-basis set effects.[149] Consequently, these studies have cast doubt on the necessity of employing self-consistent schemes within the GW framework, at least for solid-state calculations.

In Fig. 7, we report the mean signed error (MSE) and mean absolute error (MAE) associated with the principal IPs of the $GW100$ dataset[91] computed at the G_0W_0@HF and qsGW levels[135] considering the ΔCCSD(T) values as reference.[53] The distributions of the errors and the corresponding scatter plots are also provided. Going from G_0W_0@HF to qsGW lowers both the MAE from 0.31 to 0.22 eV and the MSE from −0.26 to −0.15 eV. Although the overall underestimation of GW for principal IPs remains, it is significantly reduced via the introduction of self-consistency.

4. Concluding remarks

We report an extensive review of the GW approximation within the framework of Green's function many-body perturbation theory, offering, we hope, a comprehensive analysis of both its theoretical foundations and practical applications in the context of quantum chemistry. As a starter, we introduce the concept of quasiparticles, providing a necessary backdrop for a deep dive into the derivation of Hedin's equations, a crucial starting point for our subsequent discussion on how to derive the well-established GW approximation of the self-energy.

Following this, we meticulously guide the reader through each step involved in a *GW* calculation, elucidating the panel of physical quantities that can be computed using this approach. To showcase its adaptability and effectiveness, we turn our attention to two distinct systems: the weakly correlated water molecule and the strongly correlated carbon dimer. At each stage of the process, we provide a comprehensive breakdown and offer clear explanations, complemented by numerical results and illustrative plots. The effect of self-consistency on the quasiparticle energies, which is clearly beneficial in the case of molecular systems, has been illustrated on the *GW*100 database.

The ultimate goal of this review is to facilitate the dissemination and democratization of Green's function-based formalisms within the computational and theoretical quantum chemistry community. Given the numerous successes of many-body perturbation theory across various fields of physics, quantum chemistry can certainly benefit from this formalism.[9,150] We refer the interested reader to Refs. [3–9] for more in-depth discussions around Green's function many-body perturbation theory.

Acknowledgments

We gratefully acknowledge the discussions over the years with Pina Romaniello, Arjan Berger, Fabien Bruneval, and Xavier Blase. This project has received financial support from the European Research Council (ERC) through the European Union's Horizon 2020—Research and Innovation program—under grant agreement no. 863481. Additionally, it was supported by the European Centre of Excellence in Exascale Computing (TREX), and has received funding from the European Union's Horizon 2020—Research and Innovation program—under grant agreement no. 952165.

Appendix A. Supporting information

Supplementary data associated with this article can be found in the online version at https://doi.org/10.1016/bs.aiq.2024.04.001.

References

1. Mattuck, R. D. *A guide to Feynman Diagrams in the Many-body Problem,Dover Books on Physics and Chemistry;* 2nd ed.; Dover Publications: New York, 1992.
2. Hedin, L. New Method for Calculating the One-particle Green's Function with Application to the Electron-gas Problem. *Phys. Rev.* **1965,** *139*, A796.
3. Aryasetiawan, F.; Gunnarsson, O. The GW Method. *Rep. Prog. Phys.* **1998,** *61*, 237–312.
4. Onida, G.; Reining, L.; Rubio, A. Electronic Excitations: Density-functional Versus Many-body Green's Function Approaches. *Rev. Mod. Phys.* **2002,** *74*, 601–659.
5. Reining, L. The GW Approximation: Content, Successes and Limitations: The GW Approximation. *WIREs Comput. Mol. Sci.* **2017,** *8*, e1344.

6. Golze, D.; Dvorak, M.; Rinke, P. The GW Compendium: A Practical Guide to Theoretical Photoemission Spectroscopy. *Front. Chem.* **2019,** 7, 377.
7. Martin, R. M.; Reining, L.; Ceperley, D. M. *Interacting Electrons: Theory and Computational Approaches;* Cambridge University Press, 2016.
8. Csanak, G.; Taylor, H.; Yaris, R. *Green's Function Technique in Atomic and Molecular Physics. Advances in Atomic and Molecular Physics;* Elsevier, 1971; pp. 287–361. Vol. 7.
9. Fetter, A. L.; Walecka, J. D. *Quantum Theory of Many Particle Systems;* McGraw Hill: San Francisco, 1971.
10. Starke, R.; Kresse, G. Self-Consistent Green Function Equations and the Hierarchy of Approximations for the Four-point Propagator. *Phys. Rev. B* **2012,** *85*, 075119.
11. Maggio, E.; Kresse, G. GW Vertex Corrected Calculations for Molecular Systems. *J. Chem. Theory Comput.* **2017,** *13*, 4765–4778.
12. Orlando, R.; Romaniello, P.; Loos, P.-F. Exploring New Exchange-correlation Kernels in the Bethe–Salpeter Equation: A Study of the Asymmetric Hubbard Dimer. *Adv. Quantum Chem* **2023,** *88*, 183–211.
13. Orlando, R.; Romaniello, P.; Loos, P.-F. The Three Channels of Many-Body Perturbation Theory: GW, Particle–particle, and Electron–Hole T-matrix Self-Energies. *J. Chem. Phys.* **2023,** *159*, 184113.
14. Romaniello, P.; Bechstedt, F.; Reining, L. Beyond the GW Approximation: Combining Correlation Channels. *Phys. Rev. B* **2012,** *85*, 155131.
15. Martin, P. C.; Schwinger, J. Theory of Many-Particle Systems. I. *Phys. Rev.* **1959,** *115*, 1342–1373.
16. DelSole, R.; Reining, L.; Godby, R. W. GwΓ Approximation for Electron Self-energies in Semiconductors and Insulators. *Phys. Rev. B* **1994,** *49*, 8024–8028.
17. Shirley, E. L. Self-consistent GW and Higher-order Calculations of Electron States in Metals. *Phys. Rev. B* **1996,** *54*, 7758–7764.
18. Schindlmayr, A.; Godby, R. W. Systematic Vertex Corrections Through Iterative Solution of Hedin's Equations Beyond the GW Approximation. *Phys. Rev. Lett.* **1998,** *80*, 1702.
19. Morris, A. J.; Stankovski, M.; Delaney, K. T.; Rinke, P.; García-González, P.; Godby, R. W. Vertex Corrections in Localized and Extended Systems. *Phys. Rev. B* **2007,** *76*, 155106.
20. Shishkin, M.; Marsman, M.; Kresse, G. Accurate Quasiparticle Spectra from Self-consistent GW Calculations with Vertex Corrections. *Phys. Rev. Lett.* **2007,** *99*, 246403.
21. Romaniello, P.; Guyot, S.; Reining, L. The Self-Energy Beyond GW: Local and Nonlocal Vertex Corrections. *J. Chem. Phys.* **2009,** *131*, 154111.
22. Grüneis, A.; Kresse, G.; Hinuma, Y.; Oba, F. Ionization Potentials of Solids: The Importance of Vertex Corrections. *Phys. Rev. Lett.* **2014,** *112*, 096401.
23. Hung, L.; Bruneval, F.; Baishya, K.; Öğüt, S. Benchmarking the *GW* Approximation and Bethe–Salpeter Equation for Groups IB and IIB Atoms and Monoxides. *J. Chem. Theory Comput.* **2017,** *13*, 2135–2146.
24. Cunningham, B.; Grüning, M.; Azarhoosh, P.; Pashov, D.; van Schilfgaarde, M. Effect of Ladder Diagrams on Optical Absorption Spectra in a Quasiparticle Self-consistent *GW* Framework. *Phys. Rev. Mater.* **2018,** *2*, 034603.
25. Vlček, V. Stochastic Vertex Corrections: Linear Scaling Methods for Accurate Quasiparticle Energies. *J. Chem. Theory Comput.* **2019,** *15*, 6254–6266.
26. Lewis, A. M.; Berkelbach, T. C. Vertex Corrections to the Polarizability Do Not Improve the GW Approximation for the Ionization Potential of Molecules. *J. Chem. Theory Comput.* **2019,** *15*, 2925.
27. Pavlyukh, Y.; Stefanucci, G.; van Leeuwen, R. Dynamically Screened Vertex Correction to *GW*. *Phys. Rev. B* **2020,** *102*, 045121.

28. Wang, Y.; Rinke, P.; Ren, X. Assessing the $G0W0\Gamma0(1)$ Approach: Beyond G0W0 with Hedin's Full Second-order Self-energy Contribution. *J. Chem. Theory Comput.* **2021,** *17*, 5140–5154.
29. Bruneval, F.; Dattani, N.; van Setten, M. J. The gw Miracle in Many-body Perturbation Theory for the Ionization Potential of Molecules. *Front. Chem.* **2021,** *9*, 749779.
30. Mejuto-Zaera, C.; Vlček, V. C. V. Self-Consistency in GWΓ Formalism Leading to Quasiparticle-quasiparticle Couplings. *Phys. Rev. B* **2022,** *106*, 165129.
31. Wang, Y.; Ren, X. Vertex Effects in Describing the Ionization Energies of the First-Row Transition-Metal Monoxide Molecules. *J. Chem. Theory Comput.* **2022,** *157*, 214115.
32. Förster, A.; Visscher, L. Exploring the Statically Screened G3W2 Correction to the GW Self-Energy: Charged Excitations and Total Energies of Finite Systems. *Phys. Rev. B* **2022,** *105*, 125121.
33. Bohm, D.; Pines, D. A Collective Description of Electron Interactions. I. Magnetic Interactions. *Phys. Rev.* **1951,** *82*, 625–634.
34. Pines, D.; Bohm, D. A Collective Description of Electron Interactions: II. Collective vs Individual Particle Aspects of the Interactions. *Phys. Rev.* **1952,** *85*, 338–353.
35. Bohm, D.; Pines, D. A Collective Description of Electron Interactions: III. Coulomb Interactions in a Degenerate Electron Gas. *Phys. Rev.* **1953,** *92*, 609–625.
36. Nozières, P.; Pines, D. Correlation Energy of a Free Electron Gas. *Phys. Rev.* **1958,** *111*, 442–454.
37. Loos, P. F.; Scemama, A.; Blondel, A.; Garniron, Y.; Caffarel, M.; Jacquemin, D. A Mountaineering Strategy to Excited States: Highly-Accurate Reference Energies and Benchmarks. *J. Chem. Theory Comput.* **2018,** *14*, 4360.
38. Loos, P.-F.; Boggio-Pasqua, M.; Scemama, A.; Caffarel, M.; Jacquemin, D. Reference Energies for Double Excitations. *J. Chem. Theory Comput.* **2019,** *15*, 1939–1956.
39. Véril, M.; Scemama, A.; Caffarel, M.; Lipparini, F.; Boggio-Pasqua, M.; Jacquemin, D.; Loos, P.-F. Questdb: A Database of Highly Accurate Excitation Energies for the Electronic Structure Community. *WIREs Comput. Mol. Sci.* **2021,** *11*, e1517.
40. Szabo, A.; Ostlund, N. S. *Modern Quantum Chemistry;* McGraw-Hill: New York, 1989.
41. Bruneval, F.; Marques, M. A. L. Benchmarking the Starting Points of the *GW* Approximation for Molecules. *J. Chem. Theory Comput.* **2013,** *9*, 324–329.
42. Gui, X.; Holzer, C.; Klopper, W. Accuracy Assessment of GW Starting Points for Calculating Molecular Excitation Energies using the Bethe–salpeter Formalism. *J. Chem. Theory Comput.* **2018,** *14*, 2127–2136.
43. Li, J.; Jin, Y.; Rinke, P.; Yang, W.; Golze, D. Benchmark of GW Methods for Core-Level Binding Energies. *J. Chem. Theory Comput.* **2022,** *18*, 7570–7585.
44. McKeon, C. A.; Hamed, S. M.; Bruneval, F.; Neaton, J. B. An Optimally Tuned Range-separated Hybrid Starting Point for ab Initio GW Plus Bethe–Salpeter Equation Calculations of Molecules. *J. Chem. Phys.* **2022,** *157*, 074103.
45. Blase, X.; Attaccalite, C. Charge-Transfer Excitations in Molecular Donor-acceptor Complexes within the Many-body Bethe-salpeter Approach. *Appl. Phys. Lett.* **2011,** *99*, 171909.
46. Blase, X.; Duchemin, I.; Jacquemin, D. The Bethe–Salpeter Equation in Chemistry: Relations with TD-DFT, Applications and Challenges. *Chem. Soc. Rev.* **2018,** *47*, 1022–1043.
47. Duchemin, I.; Blase, X. Robust Analytic-Continuation Approach to Many-Body GW Calculations. *J. Chem. Theory Comput.* **2020,** *16*, 1742–1756.

48. Duchemin, I.; Blase, X. Cubic-Scaling All-electron GW Calculations with A Separable Density-Fitting Space–Time Approach. *J. Chem. Theory Comput.* **2021,** *17*, 2383–2393.
49. Bruneval, F.; Rangel, T.; Hamed, S. M.; Shao, M.; Yang, C.; Neaton, J. B. Molgw 1: Many-Body Perturbation Theory Software for Atoms, Molecules, and Clusters. *Comput. Phys. Commun.* **2016,** *208*, 149–161.
50. van Setten, M. J.; Weigend, F.; Evers, F. The *GW* -Method for Quantum Chemistry Applications: Theory and Implementation. *J. Chem. Theory Comput.* **2013,** *9*, 232–246.
51. Kaplan, F.; Weigend, F.; Evers, F.; van Setten, M. J. Off-Diagonal Self-Energy Terms and Partially Self-Consistency in *GW* Calculations for Single Molecules: Efficient Implementation and Quantitative Effects on Ionization Potentials. *J. Chem. Theory Comput.* **2015,** *11*, 5152–5160.
52. Kaplan, F.; Harding, M. E.; Seiler, C.; Weigend, F.; Evers, F.; van Setten, M. J. Quasi-Particle Self-Consistent *GW* for Molecules. *J. Chem. Theory Comput.* **2016,** *12*, 2528–2541.
53. Krause, K.; Klopper, W. Implementation of the Bethe-Salpeter Equation in the Turbomole Program. *J. Comput. Chem.* **2017,** *38*, 383–388.
54. Förster, A.; Visscher, L. Quasiparticle Self-Consistent GW-Bethe–Salpeter Equation Calculations for Large Chromophoric Systems. *J. Chem. Theory Comput.* **2022,** *18*, 6779–6793.
55. Förster, A.; Visscher, L. Low-Order Scaling Quasiparticle Self-Consistent GW for Molecules. *Front. Chem.* **2021,** *9*, 736591.
56. Förster, A.; Visscher, L. Low-Order Scaling G_0W_0 by Pair Atomic Density Fitting. *J. Chem. Theory Comput.* **2020,** *16*, 7381–7399.
57. Caruso, F.; Rinke, P.; Ren, X.; Scheffler, M.; Rubio, A. Unified Description of Ground and Excited States of Finite Systems: The Self-Consistent GW Approach. *Phys. Rev. B* **2012,** *86*, 081102(R).
58. Caruso, F.; Rohr, D. R.; Hellgren, M.; Ren, X.; Rinke, P.; Rubio, A.; Scheffler, M. Bond Breaking and Bond Formation: How Electron Correlation is Captured in Many-Body Perturbation Theory and Density-Functional Theory. *Phys. Rev. Lett.* **2013,** *110*, 146403.
59. Caruso, F.; Rinke, P.; Ren, X.; Rubio, A.; Scheffler, M. Self-Consistent GW: All-Electron Implementation with Localized Basis Functions. *Phys. Rev. B* **2013,** *88*, 075105.
60. Caruso, F. Self-Consistent GW Approach for the Unified Description of Ground and Excited States of Finite Systems, PhD Thesis, Freie Universität Berlin, 2013.
61. Patterson, C. H. Exciton: A Code for Excitations in Materials. *Mol. Phys.* **2010,** *108*, 3181–3188.
62. Patterson, C. H. Photoabsorption Spectra of Small Na Clusters: TDHF and BSE Versus CI and Experiment. *Phys. Rev. Mater.* **2019,** *3*, 043804.
63. Patterson, C. H. Density Fitting in Periodic Systems: Application to TDHF in Diamond and Oxides. *J. Chem. Phys.* **2020,** *153*, 064107.
64. Hofierka, J.; Cunningham, B.; Rawlins, C. M.; Patterson, C. H.; Green, D. G. Many-body Theory of Positron Binding to Polyatomic Molecules. *Nature* **2022,** *606*, 688–693.
65. Iskakov, S.; Rusakov, A. A.; Zgid, D.; Gull, E. Effect of Propagator Renormalization on the Band Gap of Insulating Solids. *Phys. Rev. B* **2019,** *100*, 085112.
66. Sun, Q.; Zhang, X.; Banerjee, S.; Bao, P.; Barbry, M.; Blunt, N. S.; Bogdanov, N. A.; Booth, G. H.; Chen, J.; Cui, Z.-H.; Eriksen, J. J.; Gao, Y.; Guo, S.; Hermann, J.; Hermes, M. R.; Koh, K.; Koval, P.; Lehtola, S.; Li, Z.; Liu, J.; Mardirossian, N.; McClain, J. D.; Motta, M.; Mussard, B.; Pham, H. Q.; Pulkin, A.; Purwanto, W.;

Robinson, P. J.; Ronca, E.; Sayfutyarova, E. R.; Scheurer, M.; Schurkus, H. F.; Smith, J. E. T.; Sun, C.; Sun, S.-N.; Upadhyay, S.; Wagner, L. K.; Wang, X.; White, A.; Whitfield, J. D.; Williamson, M. J.; Wouters, S.; Yang, J.; Yu, J. M.; Zhu, T.; Berkelbach, T. C.; Sharma, S.; Sokolov, A. Y.; Chan, G. K.-L. Recent Developments in the PySCF Program Package. *J. Chem. Phys.* **2020,** *153*, 024109.
67. Scott, C. J. C.; Backhouse, O. J.; Booth, G. H. A "Moment-Conserving" Reformulation of GW Theory. *J. Chem. Phys.* **2023,** *158*, 124102.
68. Holzer, C.; Teale, A. M.; Hampe, F.; Stopkowicz, S.; Helgaker, T.; Klopper, W. GW Quasiparticle Energies of Atoms in Strong Magnetic Fields. *J. Chem. Phys.* **2019,** *150*, 214112.
69. Ring, P.; Schuck, P. *The Nuclear Many-Body Problem;* Springer, 2004.
70. Chen, W.; Pasquarello, A. Accurate Band Gaps of Extended Systems Via Efficient Vertex Corrections in GW. *Phys. Rev. B* **2015,** *92*, 041115.
71. Ren, X.; Marom, N.; Caruso, F.; Scheffler, M.; Rinke, P. Beyond the G W Approximation: A Second-Order Screened Exchange Correction. *Phys. Rev. B* **2015,** *92*, 081104.
72. Sawada, K. Correlation Energy of an Electron Gas at High Density. *Phys. Rev.* **1957,** *106*, 372–383.
73. Rowe, D. J. Methods for Calculating Ground-state Correlations of Vibrational Nuclei. *Phys. Rev.* **1968,** *175*, 1283.
74. Scuseria, G. E.; Henderson, T. M.; Sorensen, D. C. The Ground State Correlation Energy of the Random Phase Approximation from a Ring Coupled Cluster Doubles Approach. *J. Chem. Phys.* **2008,** *129*, 231101.
75. Furche, F. Developing the Random Phase Approximation into a Practical post-Kohn–Sham Correlation Model. *J. Chem. Phys.* **2008,** *129*, 114105.
76. Jansen, G.; Liu, R.-F.; Ángyán, J. G. On the Equivalence of Ring-Coupled Cluster and Adiabatic Connection Fluctuation-dissipation Theorem Random Phase Approximation Correlation Energy Expressions. *J. Chem. Phys.* **2010,** *133*, 154106.
77. Angyan, J. G.; Liu, R.-F.; Toulouse, J.; Jansen, G. Correlation Energy Expressions from the Adiabatic-Connection Fluctuation Dissipation Theorem Approach. *J. Chem. Theory Comput.* **2011,** *7*, 3116–3130.
78. Seeger, R.; Pople, J. A. Self-consistent Molecular Orbital Methods. XVIII. Constraints and Stability in Hartree–Fock Theory. *J. Chem. Phys.* **1977,** *66*, 3045–3050.
79. Davidson, E. R. The Iterative Calculation of a Few of the Lowest Eigenvalues and Corresponding Eigenvectors of Large Real-symmetric Matrices. *J. Comput. Phys.* **1975,** *17*, 87–94.
80. Neuhauser, D.; Rabani, E.; Baer, R. Expeditious Stochastic Calculation of Random-Phase Approximation Energies for Thousands of Electrons in Three Dimensions. *J. Phys. Chem. Lett.* **2013,** *4*, 1172–1176.
81. Govoni, M.; Galli, G. Large Scale GW Calculations. *J. Chem. Theory Comput.* **2015,** *11*, 2680–2696.
82. Liu, P.; Kaltak, M.; Klimeš, J. C. V.; Kresse, G. Cubic Scaling GW: Towards Fast Quasiparticle Calculations. *Phys. Rev. B* **2016,** *94*, 165109.
83. Vlček, V.; Rabani, E.; Neuhauser, D.; Baer, R. Stochastic GW Calculations for Molecules. *J. Chem. Theory Comput.* **2017,** *13*, 4997–5003.
84. Wilhelm, J.; Golze, D.; Talirz, L.; Hutter, J.; Pignedoli, C. A. Toward GW Calculations on Thousands of Atoms. *J. Phys. Chem. Lett.* **2018,** *9*, 306–312.
85. Duchemin, I.; Blase, X. Separable Resolution-of-the-Identity with All-Electron Gaussian Bases: Application to Cubic-Scaling RPA. *J. Chem. Phys.* **2019,** *150*, 174120.

86. Ben, M. D.; da Jornada, F. H.; Canning, A.; Wichmann, N.; Raman, K.; Sasanka, R.; Yang, C.; Louie, S. G.; Deslippe, J. Large-scale GW Calculations on Pre-Exascale HPC Systems. *Comp. Phys. Comm.* **2019,** *235*, 187–195.
87. Panadés-Barrueta, R. L.; Golze, D. Accelerating Core-level GW Calculations by Combining the Contour Deformation Approach with the Analytic Continuation of *W*. *J. Chem. Theory Comput.* **2023,** *19*, 5450–5464.
88. A Broadening Parameter of 1 eV has been Applied (2024).
89. Larson, P.; Dvorak, M.; Wu, Z. Role of the Plasmon-pole Model in the GW Approximation. *Phys. Rev. B* **2013,** *88*, 125205.
90. Deslippe, J.; Samsonidze, G.; Strubbe, D. A.; Jain, M.; Cohen, M. L.; Louie, S. G. Berkeleygw: A Massively Parallel Computer Package for the Calculation of the Quasiparticle and Optical Properties of Materials and Nanostructures. *Comput. Phys. Commun.* **2012,** *183*, 1269.
91. van Setten, M. J.; Caruso, F.; Sharifzadeh, S.; Ren, X.; Scheffler, M.; Liu, F.; Lischner, J.; Lin, L.; Deslippe, J. R.; Louie, S. G.; Yang, C.; Weigend, F.; Neaton, J. B.; Evers, F.; Rinke, P. *GW* 100: Benchmarking G_0W_0 for Molecular Systems. *J. Chem. Theory Comput.* **2015,** *11*, 5665–5687.
92. Strinati, G.; Mattausch, H. J.; Hanke, W. Dynamical Correlation Effects on the Quasiparticle Bloch States of a Covalent Crystal. *Phys. Rev. Lett.* **1980,** *45*, 290–294.
93. Hybertsen, M. S.; Louie, S. G. First-Principles Theory of Quasiparticles: Calculation of Band Gaps in Semiconductors and Insulators. *Phys. Rev. Lett.* **1985,** *55*, 1418–1421.
94. Godby, R. W.; Schlüter, M.; Sham, L. J. Self-Energy Operators and Exchange-Correlation Potentials in Semiconductors. *Phys. Rev. B* **1988,** *37*, 10159–10175.
95. vonderLinden, W.; Horsch, P. Precise Quasiparticle Energies and Hartree-Fock Bands of Semiconductors and Insulators. *Phys. Rev. B* **1988,** *37*, 8351–8362.
96. Northrup, J. E.; Hybertsen, M. S.; Louie, S. G. Many-Body Calculation of The Surface-State Energies for Si(111)2 × 1. *Phys. Rev. Lett.* **1991,** *66*, 500–503.
97. Blase, X.; Zhu, X.; Louie, S. G. Self-Energy Effects on the Surface-State Energies of H-Si(111)1 × 1. *Phys. Rev. B* **1994,** *49*, 4973–4980.
98. Rohlfing, M.; Krüger, P.; Pollmann, J. Efficient Scheme For GW Quasiparticle Band-Structure Calculations with Aapplications to Bulk Si and to the Si(001)-(2 × 1) Surface. *Phys. Rev. B* **1995,** *52*, 1905–1917.
99. Hybertsen, M. S.; Louie, S. G. Electron Correlation in Semiconductors and Insulators: Band Gaps and Quasiparticle Energies. *Phys. Rev. B* **1986,** *34*, 5390–5413.
100. Shishkin, M.; Kresse, G. Self-Consistent GW Calculations for Semiconductors and Insulators. *Phys. Rev. B* **2007,** *75*, 235102.
101. Faber, C.; Attaccalite, C.; Olevano, V.; Runge, E.; Blase, X. First-Principles GW Calculations for DNA and RNA Nucleobases. *Phys. Rev. B* **2011,** *83*, 115123.
102. Rangel, T.; Hamed, S. M.; Bruneval, F.; Neaton, J. B. Evaluating the GW Approximation with CCSD(T) for Charged Excitations Across the Oligoacenes. *J. Chem. Theory Comput.* **2016,** *12*, 2834–2842.
103. Faleev, S. V.; van Schilfgaarde, M.; Kotani, T. All-Electron Self-Consistent GW Approximation: Application to Si, MnO, and NiO. *Phys. Rev. Lett.* **2004,** *93*, 126406.
104. van Schilfgaarde, M.; Kotani, T.; Faleev, S. Quasiparticle Self-Consistent GW Theory. *Phys. Rev. Lett.* **2006,** *96*, 226402.
105. Kotani, T.; van Schilfgaarde, M.; Faleev, S. V. Quasiparticle Self-Consistent GW Method: A Basis for the Independent-Particle Approximation. *Phys. Rev. B* **2007,** *76*, 165106.
106. Ke, S.-H. All-electron GW Methods Implemented in Molecular Orbital Space: Ionization Energy and Electron Affinity of Conjugated Molecules. *Phys. Rev. B* **2011,** *84*, 205415.

107. Marie, A.; Loos, P.-F. A Similarity Renormalization Group Approach to Green's Function Methods. *J. Chem. Theory Comput.* **2023,** *19*, 3943–3957.
108. Koval, P.; Foerster, D.; Sánchez-Portal, D. Fully Self-Consistent GW and Quasiparticle Self-consistent GW for Molecules. *Phys. Rev. B* **2014,** *89*, 155417.
109. Grumet, M.; Liu, P.; Kaltak, M.; Klimeš, J. C. V.; Kresse, G. Beyond the Quasiparticle Approximation: Fully Self-Consistent GW Calculations. *Phys. Rev. B* **2018,** *98*, 155143.
110. DiSabatino, S.; Loos, P.-F.; Romaniello, P. Scrutinizing GW-Based Methods using the Hubbard Dimer. *Front. Chem.* **2021,** *9*, 751054.
111. Yeh, C.-N.; Iskakov, S.; Zgid, D.; Gull, E. Fully Self-consistent Finite-temperature GW in Gaussian Bloch Orbitals for Solids. *Phys. Rev. B* **2022,** *106*, 235104.
112. Galitskii, V.; Migdal, A. Applications of Quantum Field Theory to the Many Body Problem. *Sov. Phys. JETP* **1958,** 7, 96.
113. Stan, A.; Dahlen, N. E.; van Leeuwen, R. Fully Self-Consistent *GW* Calculations for Atoms and Molecules. *Europhys. Lett. EPL* **2006,** *76*, 298–304.
114. Pokhilko, P.; Yeh, C.-N.; Zgid, D. Iterative Subspace Algorithms for Finite-Temperature Solution of Dyson Equation. *J. Chem. Phys.* **2022,** *156*, 094101.
115. Pokhilko, P.; Iskakov, S.; Yeh, C.-N.; Zgid, D. Evaluation of Two-particle Properties within Finite-Temperature Self-Consistent One-Particle Green's Function Methods: Theory and Application to GW And GF2. *J. Chem. Phys.* **2021,** *155*, 024119.
116. Pokhilko, P.; Zgid, D. Interpretation of Multiple Solutions in Fully Iterative GF2 And GW Schemes Using Local Analysis of Two-particle Density Matrices. *J. Chem. Phys.* **2021,** *155*, 024101.
117. Bruneval, F.; Rodriguez-Mayorga, M.; Rinke, P.; Dvorak, M. Improved One-shot Total Energies from the Linearized GW Density Matrix. *J. Chem. Theory Comput.* **2021,** *17*, 2126–2136.
118. Loos, P. F.; Romaniello, P.; Berger, J. A. Green Functions and Self-Consistency: Insights from the Spherium Model. *J. Chem. Theory Comput.* **2018,** *14*, 3071–3082.
119. Ren, X.; Rinke, P.; Scuseria, G. E.; Scheffler, M. Renormalized Second-Order Perturbation Theory for the Electron Correlation Energy: Concept, Implementation, and Benchmarks. *Phys. Rev. B* **2013,** *88*, 035120.
120. Luttinger, J. M.; Ward, J. C. Ground-State Energy of a Many-Fermion System. II. *Phys. Rev.* **1960,** *118*, 1417–1427.
121. Klein, A. Perturbation Theory for an Infinite Medium of Fermions. II. *Phys. Rev.* **1961,** *121*, 950–956.
122. Dahlen, N. E.; van Leeuwen, R.; vonBarth, U. Variational Energy Functionals of the Green Function and of the Density Tested on Molecules. *Phys. Rev. A* **2006,** *73*, 012511.
123. Dahlen, N. E.; Van Leeuwen, R.; VonBarth, U. Variational Energy Functionals of the Green Function Tested on Molecules. *Int. J. Quantum Chem.* **2005,** *101*, 512–519.
124. Dahlen, N. E.; van Leeuwen, R. Self-Consistent Solution of the Dyson Equation for Atoms and Molecules within a Conserving Approximation. *J. Chem. Phys.* **2005,** *122*, 164102.
125. Dahlen, N. E.; von Barth, U. Variational Second-order Møller–Plesset Theory Based on the Luttinger–Ward Functional. *J. Chem. Phys.* **2004,** *120*, 6826–6831.
126. Dahlen, N. E.; vonBarth, U. Variational Energy Functionals Tested on Atoms. *Phys. Rev. B* **2004,** *69*, 195102.
127. Stan, A.; Dahlen, N. E.; van Leeuwen, R. Levels of Self-Consistency in the GW Approximation. *J. Chem. Phys.* **2009,** *130*, 114105.
128. Maggio, E.; Liu, P.; van Setten, M. J.; Kresse, G. *GW* 100: A Plane Wave Perspective for Small Molecules. *J. Chem. Theory Comput.* **2017,** *13*, 635–648.

129. Véril, M.; Romaniello, P.; Berger, J. A.; Loos, P. F. Unphysical Discontinuities in GW Methods. *J. Chem. Theory Comput.* **2018,** *14*, 5220.
130. A. Marie, P.-F. Loos, Reference energies for valence ionizations and satellite transitions (2024), arXiv:2402.13877 [physics.chem-ph].
131. Garniron, Y.; Gasperich, K.; Applencourt, T.; Benali, A.; Ferté, A.; Paquier, J.; Pradines, B.; Assaraf, R.; Reinhardt, P.; Toulouse, J.; Barbaresco, P.; Renon, N.; David, G.; Malrieu, J. P.; Véril, M.; Caffarel, M.; Loos, P. F.; Giner, E.; Scemama, A. Quantum Package 2.0: A Open-source Determinant-Driven Suite of Programs. *J. Chem. Theory Comput.* **2019,** *15*, 3591.
132. Johnson, R. Computational Chemistry Comparison and Benchmark Database. *NIST Standard Reference Database* **2002,** *101*.
133. Pavlyukh, Y.; Hübner, W. Configuration Interaction Approach for the Computation of the Electronic Self-Energy. *Phys. Rev. B* **2007,** *75*, 205129.
134. Ammar, A.; Marie, A.; Rodríguez-Mayorga, M.; Burton, H.G.A.; Loos, P.-F. Can GW Handle Multireference Systems? **2024**, arxiv:2401.03745.
135. Caruso, F.; Dauth, M.; van Setten, M. J.; Rinke, P. Benchmark of GW Approaches for the GW100 Test Set. *J. Chem. Theory Comput.* **2016,** *12*, 5076.
136. Hung, L.; da Jornada, F. H.; Souto-Casares, J.; Chelikowsky, J. R.; Louie, S. G.; Öğüt, S. Excitation Spectra of Aromatic Molecules within a Real-space GW-BSE Formalism: Role of Self-Consistency and Vertex Corrections. *Phys. Rev. B* **2016,** *94*, 085125.
137. Jacquemin, D.; Duchemin, I.; Blase, X. Is the Bethe–Salpeter Formalism Accurate for Excitation Energies? Comparisons with TD-DFT, CASPT2, and EOM-CCSD. *J. Phys. Chem. Lett.* **2017,** *8*, 1524–1529.
138. Rostgaard, C.; Jacobsen, K. W.; Thygesen, K. S. Fully Self-Consistent GW Calculations for Molecules. *Phys. Rev. B* **2010,** *81*, 085103.
139. Holm, B.; von Barth, U. Fully Self-Consistent GW Self-Energy of the Electron Gas. *Phys. Rev. B* **1998,** *57*, 2108.
140. Holm, B. Total Energies from GW Calculations. *Phys. Rev. Lett.* **1999,** *83*, 788–791.
141. Holm, B.; Aryasetiawan, F. Total Energy from the Galitskii-migdal Formula Using Realistic Spectral Functions. *Phys. Rev. B* **2000,** *62*, 4858.
142. García-González, P.; Godby, R. W. Self-Consistent Calculation of Total Energies of the Electron Gas Using Many-body Perturbation Theory. *Phys. Rev. B* **2001,** *63*, 075112.
143. Loos, P.-F.; Gill, P. M. W. The Uniform Electron Gas. *Wiley Interdiscip. Rev. Comput. Mol. Sci.* **2016,** *6*, 410–429.
144. Schöne, W.-D.; Eguiluz, A. G. Self-Consistent Calculations of Quasiparticle States in Metals and Semiconductors. *Phys. Rev. Lett.* **1998,** *81*, 1662–1665.
145. Ku, W.; Eguiluz, A. G. Band-Gap Problem in Semiconductors Revisited: Effects of Core States and Many-Body Self-Consistency. *Phys. Rev. Lett.* **2002,** *89*, 126401.
146. Kutepov, A. L. Electronic Structure of Na, K, Si, and LiF from Self-Consistent Solution of Hedin's Equations Including Vertex Corrections. *Phys. Rev. B* **2016,** *94*, 155101.
147. Kutepov, A. L.; Kotliar, G. One-Electron Spectra and Susceptibilities of the Three-dimensional Electron Gas from Self-consistent Solutions of Hedin's Equations. *Phys. Rev. B* **2017,** *96*, 035108.
148. de Groot, H. J.; Bobbert, P. A.; van Haeringen, W. Self-Consistent *GW* for a Quasi-One-dimensional Semiconductor. *Phys. Rev. B* **1995,** *52*, 11000–11007.
149. Friedrich, C.; Schindlmayr, A.; Blügel, S.; Kotani, T. Elimination of the Linearization Error in GW Calculations Based on the Linearized Augmented-plane-Wave Method. *Phys. Rev. B* **2006,** *74*, 045104.
150. DickHoff, W. H.; Neck, D. V. *Many-Body Theory Exposed!;* World Scientific, 2008.